

Short-Range MIMO Throughput Prediction Based on Spherical Wave Model

Jianchuan Wei¹, Xiaoyu Huang¹, Chongwen Huang², Member, IEEE, Wei E.I. Sha¹, Senior Member, IEEE, and Xiaoming Chen¹, Senior Member, IEEE

Abstract—The exploration of Internet-of-Things (IoT) has led to widespread short-range multiple-input–multiple-output (MIMO) communications. However, traditional throughput models, limited by the far-field propagation assumptions, often fail to accurately evaluate the spatial multiplexing capability and throughput performance in short-range line-of-sight (LOS) scenarios. Against this backdrop, this letter reveals the limitations of the conventional plane wave model-based throughput model from the perspective of the effective degree of freedom (EDOF) and develops a MIMO throughput model for short-range LOS scenarios using a spherical wave model (SWM). The relationship between EDOF and throughput is analyzed and discussed. Our results show that EDOF can effectively indicate throughput variations across different transceiver layouts in short-range LOS scenarios. Throughput measurements of MIMO devices are conducted to show the superiority of the proposed SWM-based throughput model to the traditional one.

Index Terms—Antennas, multiple-input–multiple-output (MIMO), short-range communication, spherical wave model, throughput.

I. INTRODUCTION

WITH the continuous advancements in ultra-massive multiple-input–multiple-output (MIMO), reconfigurable intelligent surfaces (RIS), millimeter-wave and terahertz communications, and Internet-of-Things (IoT) technologies [1], [2], [3], [4], [5], future wireless networks are inclined to adopt larger array apertures and dense deployment, making short-range MIMO communications increasingly popular [6].

However, the increase in communication frequencies renders high-frequency signals more susceptible to path loss and atmospheric absorption, not only shortening the propagation distance but also reducing the signal’s penetration and diffraction capabilities [7], [8]. Consequently, line-of-sight (LOS) propagation becomes more prevalent. According to classic MIMO theory and throughput models, spatial multiplexing is inevitably impacted under LOS propagation conditions. This is because LOS conditions typically result in a unity-rank channel, which

Manuscript received 3 May 2024; accepted 23 May 2024. Date of publication 27 May 2024; date of current version 6 September 2024. This work was supported in part by the National Natural Science Foundation of China under Grant 62171362. (Corresponding author: Xiaoming Chen.)

Jianchuan Wei, Xiaoyu Huang, and Xiaoming Chen are with the School of Information and Communications Engineering, Xi'an Jiaotong University, Xi'an 710049, China (e-mail: xiaoming.chen@mail.xjtu.edu.cn).

Chongwen Huang and Wei E.I. Sha are with the College of Information Science and Electronic Engineering, Zhejiang University, Hangzhou 310027, China.

Digital Object Identifier 10.1109/LAWP.2024.3405555

cannot support the transmission of multiple parallel layers. This limitation is primarily based on the assumption of far-field propagation, where all antenna elements receive signals from the same angle and experience the same propagation path loss (i.e., plane-wave assumption).

Traditionally, the metric that distinguishes between the radiative near-field and far-field regions is known as the Fraunhofer distance [9], which primarily depends on the array aperture and the wavelength. When the transmission distance D exceeds the Fraunhofer distance, the electromagnetic field can be approximated by a plane wave model (PWM). However, for future communication systems with larger array apertures, higher carrier frequencies, and/or dense IoT deployment, D often falls below the Fraunhofer distance. In such cases, employing a PWM to mimic the electromagnetic field is not sufficiently accurate. This inadequacy further impacts the traditional PWM-based throughput model [10], [11], [12], making it challenging to accurately assess the spatial multiplexing capability and throughput performance of communication systems in short-range LOS scenarios.

In light of the PWM’s shortcomings, this work utilizes the spherical wave model (SWM) [13] to accurately model the propagation channel in short-range scenarios and develops a SWM-based throughput prediction scheme based on the threshold receiver model to accurately assess the system’s throughput. The throughput measurement of actual MIMO devices in LOS scenarios exhibits good consistency between the measured throughput and the modeled one, proving the accuracy of the proposed throughput model. Specifically, the contributions of this work are summarized as follows.

- 1) This study reveals the limitation of the conventional PWM-based throughput model in short-range LOS scenarios from the perspective of effective degree of freedom (EDOF) and develops a SWM-based throughput model, which allows for a more accurate assessment of the system’s throughput compared to traditional models.
- 2) The relationship between EDOF and throughput is analyzed and discussed for the first time in this work. EDOF not only characterizes the system’s correlation and power imbalance effectively but also indicates the relative trend of throughput changes across different transceiver layouts. This capability provides a significant advantage over the traditional antenna separation product (ASP) deviation factor (DF) model [14], [15], [16] based on the information-theoretic capacity in LOS MIMO systems, which only indicates the transceiver layout achieving maximum throughput.
- 3) The proposed SWM-based throughput model is validated by throughput measurement of actual MIMO access points

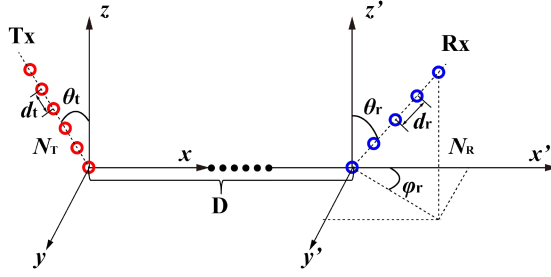


Fig. 1. Schematic layout of the transmitter-receiver.

(AP) and station (STA) in short-range LOS scenarios. This indicates that spatial multiplexing remains feasible in short-range communications due to the nonnegligible wave curvature over the array, even in pure LOS environments without scattering.

II. THEORY

A. SWM and PWM

The schematic diagram of a $N_T \times N_R$ MIMO system is shown in Fig. 1, where both the transmitting (Tx) and receiving (Rx) arrays are uniform linear arrays (ULAs) with the same polarization for better illustration. For the spherical wave model, in scenarios considering LOS transmission only, the subchannel between the s th Tx antenna and the u th Rx antenna can be modeled as

$$[\mathbf{H}_{\text{SWM}}]_{u,s} = \frac{\lambda \sqrt{G^{\text{Rx}}(\Omega_{u,s}^{\text{R}}) G^{\text{Tx}}(\Omega_{u,s}^{\text{T}})}}{4\pi d_{u,s}} e^{\frac{-j2\pi d_{u,s}}{\lambda}} \quad (1)$$

where $[\mathbf{A}]_{u,s}$ denotes the element in row i and column j ; λ denote the carrier wavelength; $d_{u,s}$ represents the Euclidean distance between s th Tx antenna and the u th Rx antenna; G^{Rx} and G^{Tx} denote the gains of the Rx and Tx antenna arrays, respectively. $\Omega_{u,s}^{\text{R}} \triangleq (\theta_{u,s}^{\text{R}}, \phi_{u,s}^{\text{R}})$ and $\Omega_{u,s}^{\text{T}} \triangleq (\theta_{u,s}^{\text{T}}, \phi_{u,s}^{\text{T}})$ denote the direction-of-arrival (DOA) and direction-of-departure (DOD) solid angles of the u th Rx and s th Tx antenna pairs.

When the distance D between transceivers is sufficiently large, the channel can be modeled using the plane wavefront approximation. At this point, the PWM channel matrix can be expressed as [17]

$$\mathbf{H}_{\text{PWM}} = \frac{\lambda \sqrt{G^{\text{Rx}}(\Omega_c^{\text{R}}) G^{\text{Tx}}(\Omega_c^{\text{T}})}}{4\pi D} e^{\frac{-j2\pi D}{\lambda}} \mathbf{a}_r(\Omega_c^{\text{R}}) \mathbf{a}_t^H(\Omega_c^{\text{T}}) \quad (2)$$

where Ω_c^{R} and Ω_c^{T} , respectively, represent the DOA and DOD at the centers of the receiving and transmitting arrays; \mathbf{a}_r and \mathbf{a}_t denote the steering vectors of the receiving and transmitting arrays, respectively; and the superscript H denotes the Hermitian transpose.

It can be observed from (2) that the channel modeled by the PWM is unity-rank, implying that the channel lacks spatial multiplexing capability.

B. Effective Degree of Freedom (EDOF)

EDOF is used in this work to more specifically assess the spatial multiplexing capability of the channels modeled by

PWM and SWM. Specifically, EDOF can effectively evaluate the number of parallel channels (i.e., equivalent single-input single-output links) and hence characterize the spatial multiplexing performance [18]. For a channel sample \mathbf{H} , the Pearson correlation can be expressed as

$$\mathbf{R}_r = \mathcal{N}(\mathbf{H}\mathbf{H}^H) \quad (3)$$

where $\mathcal{N}(\cdot)$ denotes the normalization operation, and the superscript H indicates the conjugate transpose operation. At this point, the EDOF can be represented as [19]

$$\psi_e(\mathbf{R}_r) = \left(\frac{\text{tr}(\mathbf{R}_r)}{\|\mathbf{R}_r\|_F} \right)^2 = \left(\sum_i \sigma_i \right)^2 / \sum_i \sigma_i^2 \quad (4)$$

where $\text{tr}(\cdot)$ and $\|\cdot\|_F$ denote the trace operator and Frobenius norm, respectively. σ_i indicates the i th eigenvalue of \mathbf{R}_r . Based on (2), the EDOF of the channel modeled by PWM can be expressed as

$$\psi_e^{\text{PWM}}(\mathcal{N}(\mathbf{H}_{\text{PWM}}\mathbf{H}_{\text{PWM}}^H)) = 1 \quad (5)$$

which also implies that the channel lacks spatial multiplexing capability. Similarly, the EDOF of the SWM channel can be represented as

$$\psi_e^{\text{SWM}}(\mathcal{N}(\mathbf{H}_{\text{SWM}}\mathbf{H}_{\text{SWM}}^H)) \geq 1, \text{ and } \lim_{D \rightarrow \infty} \psi_e^{\text{SWM}} = 1. \quad (6)$$

Comparing (5) and (6), it can be seen that in far-field communications, the EDOF of the channel of SWM and PWM tends to converge. However, in short-range communications, the plane wave model underestimates the EDOF of the channel. This means the conventional PWM-based throughput model would underestimate the spatial multiplexing gain of the channel, resulting in an underestimation of the MIMO system's throughput.

Furthermore, it can be observed from (4) that the EDOF can effectively reflect the channel correlation and power imbalance. Higher correlation and power imbalance lead to uneven distribution of the eigenvalues of the correlation matrix \mathbf{R}_r , which in turn reduces EDOF. Since channel correlation and power imbalance are key indicators affecting system throughput performance [20], [21], EDOF can thus serve as an effective indicator of throughput fluctuations. The simulation analysis of the relationship between EDOF and throughput is shown in the next section.

C. Throughput Model

For a $N_T \times N_R$ MIMO system under flat fading, the received signal can be represented as

$$\mathbf{y} = \mathbf{HPs} + \mathbf{n} \quad (7)$$

where $\mathbf{P} \in C^{N_T \times N_T}$ is the precoding matrix; $\mathbf{H} \in C^{N_R \times N_T}$ is the channel matrix; $\mathbf{s} \in C^{N_T \times 1}$ denotes the transmit symbol vector; $\mathbf{n} \in C^{N_R \times 1}$ is a complex additive white Gaussian noise (AWGN) with zero mean and unity variance. In the receiver, when the decoder matrix \mathbf{G} is assumed to deal with interference, the effective signal-to-noise ratio (SNR) of the i th stream (after equalization) can be expressed as

$$\gamma_i = \frac{\bar{\gamma}_0 |\mathbf{g}_i \mathbf{w}_i|^2}{\sum_{k \neq i} |\mathbf{g}_i \mathbf{w}_k|^2 + [\mathbf{G} \mathbf{G}^H]_{i,i}} \quad (8)$$

where $\bar{\gamma}_0$ denotes the transmit SNR; \mathbf{w}_i denotes the i th column vector of matrix $\mathbf{W} = \mathbf{HP}$ and \mathbf{g}_i denotes the i th row vector

of decoder matrix \mathbf{G} . Based on the throughput model proposed in [10], [11], and [22], the average block error rate (BLER) per layer of the system can be expressed as

$$\overline{\text{BLER}}(\bar{\gamma}_i) = \int_0^{\gamma_{\text{th}}} f(\gamma_i; \bar{\gamma}_i) d\gamma_i = F(\gamma_{\text{th}}; \bar{\gamma}_i) \quad (9)$$

where γ_{th} denotes the threshold value; γ_i and $\bar{\gamma}_i$ represent the received SNR and the average SNR of the i th layer; $f(\cdot)$ and $F(\cdot)$ denote the probability density function and cumulative distribution function, respectively. On this basis, the total throughput can be modeled as the sum of the throughputs of all layers

$$T_{\text{put}}(\bar{\gamma}) = \frac{T_{\text{put,max}}}{N_s} \sum_{i=1}^{N_s} (1 - \overline{\text{BLER}}(\bar{\gamma}_i)) \quad (10)$$

where $T_{\text{put,max}}$ is the maximum data rate of the system, N_s is the maximum number of layers and $\bar{\gamma}$ is the average of $\bar{\gamma}_i$. The conventional PWM-based throughput can be simplified as

$$\begin{aligned} T_{\text{put}}^{\text{PWM}}(\bar{\gamma}) &= \frac{T_{\text{put,max}}}{N_s} \sum_{i=1}^{\text{rank}(\mathbf{H}_{\text{PWM}})} (1 - \overline{\text{BLER}}(\bar{\gamma}_i)) \\ &= \frac{T_{\text{put,max}}}{N_s} (1 - \overline{\text{BLER}}(\bar{\gamma}_1)) \end{aligned} \quad (11)$$

where $\text{rank}(\cdot)$ denotes the rank-taking operator. For the SWM-based throughput, it can be obtained as

$$T_{\text{put}}^{\text{SWM}}(\bar{\gamma}) = \frac{T_{\text{put,max}}}{N_s} \sum_{i=1}^{\text{rank}(\mathbf{H}_{\text{SWM}})} (1 - \overline{\text{BLER}}(\bar{\gamma}_i)). \quad (12)$$

From (11) and (12), it can be observed that in short-range LOS scenarios, the traditional PWM-based throughput model significantly underestimates the system's spatial multiplexing gain, thereby underestimating the throughput. In this case, using the proposed SWM-based throughput model can more accurately assess the MIMO system's throughput.

III. SIMULATIONS AND EXPERIMENTAL RESULTS

In this section, firstly, we simulated a 4×4 LOS MIMO system with both Tx and Rx arrays being ULAs, placed on the same plane and parallel to each other, assuming each antenna element has an isotropic radiation pattern. We simulated the EDOF of the system as a function of distance from Tx to Rx D with different carrier frequencies f_c and antenna spacing $d_r = d_t = d$, as shown in Fig. 2(a). Additionally, the EDOF as a function of number of antennas N of Tx and Rx under a const aperture $L = 10.5\lambda_0$ with different D were also simulated, as shown in Fig. 2(b).

From Fig. 2(a), it can be observed that within the Fraunhofer distance, the EDOFs of the channel modeled by SWM are significantly greater than that of the traditional PWM. This implies that the traditional LOS channel modeling based on the PWM significantly underestimates the spatial multiplexing gain of short-range MIMO communication systems. Furthermore, it can be observed from Fig. 2(b) that as N increases, the EDOF of SWM initially increases rapidly and reaches a maximum. Thereafter, as N continues to increase, EDOF begins to decline and gradually stabilizes. This decline is primarily due to the increased system correlation caused by the decreasing distance between antennas, which offsets the increase in EDOF due to the rising number of antennas.

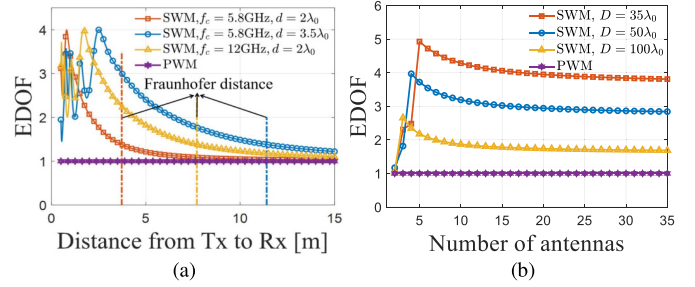


Fig. 2. EDOF (a) as a function of distance from Tx to Rx D with different carrier frequency f_c and antenna spacing d ; (b) as a function of number of antennas N under a const aperture $L = 10.5\lambda_0$ with different D . λ_0 is the wavelength corresponding to the frequency of 5.8 GHz.

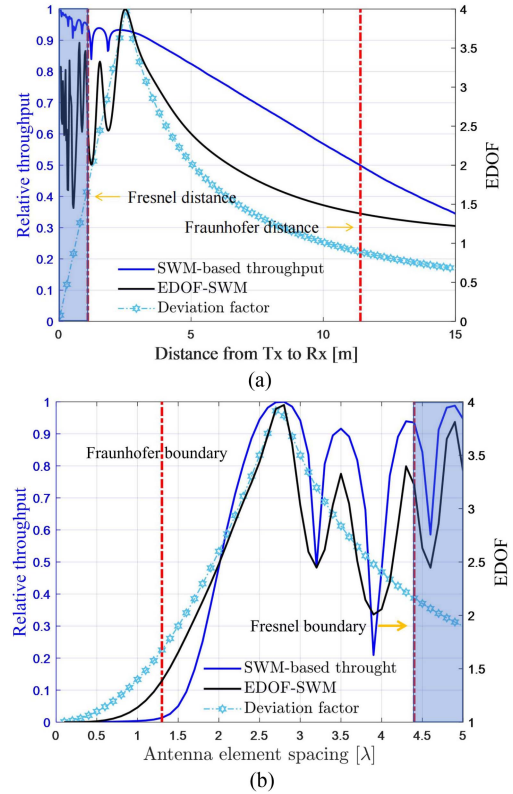


Fig. 3. SWM-based relative throughput, EDOF and DF (a) as a function of the distance between Tx and Rx with $d_r = d_t = 3.5\lambda$; and (b) as a function of the antenna spacing with $D = 30\lambda$, $f_c = 5.8$ GHz.

Additionally, we analyzed the variations in SWM-based relative throughput, EDOF, and the traditional optimum capacity-based antena separation product (ASP) DF in the above LOS MIMO systems at different transmitter-receiver distances and different antenna element spacings. The results are shown in Fig. 3.

It is noteworthy that the ASP DF is defined to evaluate the deviation of actual layout from optimal layout from the aspect of information-theoretic capacity and is given by [14], [15], and [16]

$$DF = \frac{\lambda D}{d_t d_r V \cos \theta_t \cos \theta_r}. \quad (13)$$

where $V = \max(N_T, N_R)$. It has been demonstrated in [15] that when $DF = 1$, the channel exhibits optimal orthogonality,

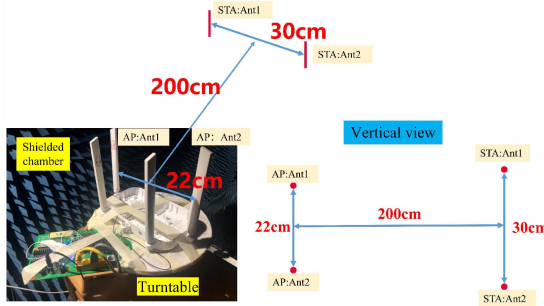


Fig. 4. Throughput measurement system schematic.

thereby achieving the maximum channel capacity. When DF deviates from 1, the channel capacity of the system decreases. For simplicity, in this work, we normalize DF as follows:

$$DF = \begin{cases} DF & (DF \leq 1) \\ \frac{1}{DF} & (DF > 1) \end{cases}. \quad (14)$$

It is observed from Fig. 3 that although the DF can adequately indicate the locations of higher throughput, it fails to accurately reflect the changes in throughput with distance and antenna spacing. In contrast, EDOF, due to its effective representation of system correlation and power imbalances, provides a more accurate indication of the fluctuations in system throughput. It is noteworthy that this work primarily focuses on short-range scenarios where the distance D exceeds the Fresnel distance $0.62\sqrt{L^3/\lambda}$. When D is less than the Fresnel distance, the presence of evanescent waves can affect the accuracy of traditional channel modeling methods.

Building upon this, we measure the throughput of actual MIMO AP and STA to further validate the proposed throughput model. The schematic of the measurement system is shown in Fig. 4, where the AP with two antenna elements is placed on a turntable in a shielded chamber, and the STA is placed parallel to it on the same horizontal plane, with a distance of 2 m. The Inter Wi-Fi 6 AX200 module is used in the STA for throughput measurement with a bandwidth of 160 MHz. During the measurement, the AP is fixed to transmit signals in 2 spatial streams, and it rotates horizontally on the turntable at intervals of 30°. The measured throughput is averaged at all rotation angles.

It should be noted that the measurement system in this work supports adaptive modulation and coding scheme (MCS) techniques. The adaptive MCS throughput with fixed k layers can be expressed as [23]

$$\begin{aligned} T_{\text{put,adpMCS}}^k(\bar{\gamma}) \\ = \max(T_{\text{put},1}^k(\bar{\gamma}), T_{\text{put},2}^k(\bar{\gamma}), \dots, T_{\text{put},M}^k(\bar{\gamma})) \end{aligned} \quad (15)$$

where $T_{\text{put},m}^k(\bar{\gamma})$ represents the throughput with fixed MCS m and k layers, which can be obtained as

$$\begin{aligned} T_{\text{put},m}^k(\bar{\gamma}) \\ = \frac{T_{\text{put,max},m}^k}{T_{\text{put,max},M}^k} \cdot T_{\text{put},M}^k[\bar{\gamma} - (\Gamma_M - \Gamma_m)] \end{aligned} \quad (16)$$

where $T_{\text{put,max},m}^k$ is the maximum throughput with fixed k layers and MCS m , Γ_m is the switching threshold SNR of MCS m when

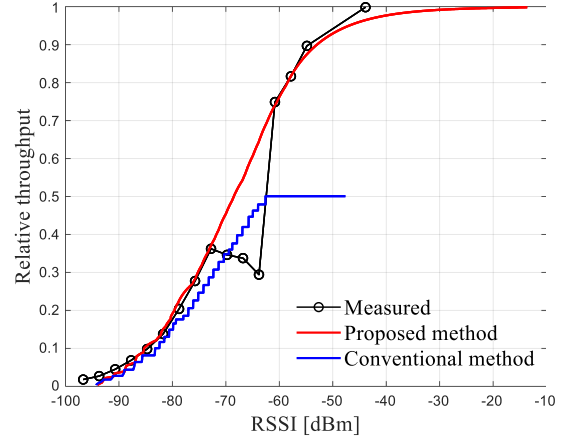


Fig. 5. Measured (black) and simulated (red: the proposed SWM-based throughput model and blue: the conventional PWM-based throughput model) throughput of actual MIMO AP and STA system.

the BLER reaches 10%. The MCS feedback lookup of the system can be obtained in [24, Table 22-55].

Fig. 5 displays the measured throughput compared with the simulated throughput. The channels of the simulation are sampled with different rotation angles of the AP to ensure consistency between the simulation settings and the measurement settings. A total of 10 000 channel drops were sampled during the simulation process. It is worth noting that the simulated throughput is, by default a function of $\bar{\gamma}$, whereas the measured throughput is a function of RSSI. To correct for the differences between simulation results and measurements, it is necessary to apply a threshold γ_{th} , as shown in (9). The γ_{th} can be obtained through conductive measurements, as described in [10] and [22].

From Fig. 5, it can be observed that the proposed SWM-based throughput model can accurately predict the short-range LOS MIMO system's throughput. However, the conventional PWM-based throughput model because it underestimates the EDOF of the system and therefore it will significantly underestimate the throughput of the system at high SNR. Additionally, the measured result demonstrates that even in environments with little or no scattering, spatial multiplexing is still feasible in short-range communications.

IV. CONCLUSION

In this letter, we analyzed the differences between the SWM and the PWM from the perspective of EDOF, revealing the significant underestimation of the system's spatial multiplexing capacity and throughput in short-range LOS scenarios by the traditional PWM-based throughput model. Building upon this, we proposed an SWM-based throughput model suitable for short-range LOS scenarios. The relationship between EDOF and SWM-based throughput is analyzed and discussed. Our results show that EDOF more effectively indicates throughput variations across different transceiver layouts in short-range LOS scenarios than the traditional ASP DF model based on the information-theoretic capacity. The throughput of actual MIMO AP and STA is measured. The simulation result of throughput aligning with the actual measurement validates the accuracy of the proposed SWM-based throughput model.

REFERENCES

- [1] A. Faisal, H. Sarieddeen, H. Dahrouj, T. Y. Al-Naffouri, and M. -S. Alouini, "Ultramassive MIMO systems at terahertz bands: Prospects and challenges," *IEEE Veh. Technol. Mag.*, vol. 15, no. 4, pp. 33–42, Dec. 2020.
- [2] G. Sun et al., "Geometric-based channel modeling and analysis for double-RIS aided vehicle-to-vehicle communication systems," *IEEE Internet Things J.*, vol. 11, no. 10, pp. 18888–18901, May 2024, doi: [10.1109/IJOT.2024.3370148](https://doi.org/10.1109/IJOT.2024.3370148).
- [3] M. S. Kildal, S. M. Moghaddam, J. Carlsson, J. Yang, and A. A. Glazunov, "Evaluation of a random line-of-sight over-the-air measurement setup at 28 GHz," *IEEE Trans. Antennas Propag.*, vol. 69, no. 8, pp. 5008–5020, Aug. 2021.
- [4] Y. Chen, R. Li, C. Han, S. Sun, and M. Tao, "Hybrid spherical- and planar-wave channel modeling and estimation for terahertz integrated UM-MIMO and IRS systems," *IEEE Trans. Wireless Commun.*, vol. 22, no. 12, pp. 9746–9761, Dec. 2023.
- [5] Y. Yuan et al., "A 3D geometry-based reconfigurable intelligent surfaces-assisted mmwave channel model for high-speed train communications," *IEEE Trans. Veh. Technol.*, vol. 73, no. 2, pp. 1524–1539, Feb. 2024, doi: [10.1109/TVT.2023.3321645](https://doi.org/10.1109/TVT.2023.3321645).
- [6] M. Cui, Z. Wu, Y. Lu, X. Wei, and L. Dai, "Near-field MIMO communications for 6G: Fundamentals, challenges, potentials, and future directions," *IEEE Commun. Mag.*, vol. 61, no. 1, pp. 40–46, Jan. 2023.
- [7] K. Li, K. Sasaki, K. Wake, T. Onishi, and S. Watanabe, "Quantitative comparison of power densities related to electromagnetic near-field exposures with safety guidelines from 6 to 100 GHz," *IEEE Access*, vol. 9, pp. 115801–115812, 2021.
- [8] X. Zhang, N. Sood, J. K. Siu, and C. D. Sarris, "A hybrid ray-tracing/vector parabolic equation method for propagation modeling in train communication channels," *IEEE Antennas Wireless Propag. Lett.*, vol. 64, no. 5, pp. 1840–1849, May 2016.
- [9] K. T. Selvan and R. Janaswamy, "Fraunhofer and Fresnel distances: Unified derivation for aperture antennas," *IEEE Antennas Propag. Mag.*, vol. 59, no. 4, pp. 12–15, Aug. 2017.
- [10] P.-S. Kildal et al., "Threshold receiver model for throughput of wireless devices with MIMO and frequency diversity measured in reverberation chamber," *IEEE Antennas Wireless Propag. Lett.*, vol. 10, pp. 1201–1204, 2011.
- [11] Y. Wang et al., "Improvement of diversity and capacity of MIMO system using scatterer array," *IEEE Trans. Antennas Propag.*, vol. 70, no. 1, pp. 789–794, Jan. 2022.
- [12] M. S. Kildal, S. Mansouri Moghaddam, A. Razavi, J. Carlsson, J. Yang, and A. Alayón Glazunov, "Verification of the random line-of-sight measurement setup at 1.5–3 GHz including MIMO throughput measurements of a complete vehicle," *IEEE Trans. Veh. Technol.*, vol. 69, no. 11, pp. 13165–13179, Nov. 2020.
- [13] Jeng-Shiann Jiang and M. A. Ingram, "Spherical wave model for short-range MIMO," *IEEE Trans. Commun.*, vol. 53, no. 9, pp. 1534–1541, Sep. 2005.
- [14] I. Sarris and A. R. Nix, "Design and performance assessment of high-capacity MIMO architectures in the presence of a line-of-sight component," *IEEE Trans. Veh. Technol.*, vol. 56, no. 4, pp. 2194–2202, Jul. 2007.
- [15] F. Bohagen, P. Orten, and G. E. Oien, "Design of optimal high-rank line-of-sight MIMO channels," *IEEE Trans. Wireless Commun.*, vol. 6, no. 4, pp. 1420–1425, Apr. 2007.
- [16] K. Murata, N. Honma, K. Nishimori, N. Michishita, and H. Morishita, "Analog eigenmode transmission for short-range MIMO based on orbital angular momentum," *IEEE Trans. Antennas Propag.*, vol. 65, no. 12, pp. 6687–6702, Dec. 2017.
- [17] F. Bohagen, P. Orten, and G. E. Oien, "On spherical vs. plane wave modeling of line-of-sight MIMO channels," *IEEE Trans. Commun.*, vol. 57, no. 3, pp. 841–849, Mar. 2009.
- [18] Y. Shen, Z. He, W. E. I. Sha, S. S. A. Yuan, and X. Chen, "Electromagnetic effective-degree-of-freedom prediction with parabolic equation method," *IEEE Trans. Antennas Propag.*, vol. 71, no. 4, pp. 3752–3757, Apr. 2023.
- [19] S. S. A. Yuan, Z. He, X. Chen, C. Huang, and W. E. I. Sha, "Electromagnetic effective degree of freedom of a MIMO system in free space," *IEEE Antennas Wireless Propag. Lett.*, vol. 21, no. 3, pp. 446–450, Mar. 2022.
- [20] X. Chen, "Throughput multiplexing efficiency for MIMO antenna characterization," *IEEE Antennas Wireless Propag. Lett.*, vol. 12, pp. 1208–1211, 2013.
- [21] X. Huang et al., "Throughput multiplexing efficiency for high-order handset MIMO antennas," *Electronics*, vol. 11, no. 9, pp. 1301, Apr. 2022.
- [22] X. Chen, W. Fan, L. Hentilä, P. Kyösti, and G. F. Pedersen, "Throughput modeling and validations for MIMO-OTA testing with arbitrary multi path," *IEEE Antennas Wireless Propag. Lett.*, vol. 17, no. 4, pp. 637–640, Apr. 2018.
- [23] J. Wei et al., "Throughput modeling and validation of MIMO terminals with adaptive MCS and layers," *IEEE Trans. Instrum. Meas.*, vol. 73, 2024, Art. no. 5501004.
- [24] ISO/IEC/IEEE International Standard, "ISO/IEC/IEEE International Standard - Information technology—Telecommunications and information exchange between systems—Local and metropolitan area networks—Specific requirements—Part 11: Wireless LAN medium access control (MAC) and physical layer (PHY) specifications AMENDMENT 4," ISO/IEC/IEEE 8802-11:2012/Amd.4:2015(E) (Adoption of IEEE Std 802.11ac-2013), pp. 1–430, Aug. 1, 2015, doi: [10.1109/IEEESTD.2015.7226764](https://doi.org/10.1109/IEEESTD.2015.7226764).